

## Growth in non-Laplacian fields

A. P. Roberts and M. A. Knackstedt

*Department of Applied Mathematics, Research School of Physical Sciences and Engineering, Australian National University,  
GPO Box 4, Canberra, Australian Capital Territory 2601, Australia*

(Received 31 July 1992)

We develop a formal method for assigning rules to lattice-based walkers which allows the modeling of irreversible growth in systems governed by non-Laplacian partial differential equations. The method is used to study diffusive growth in finite concentration fields. Good agreement with analytic results is obtained. The method is subsequently applied to study electrochemical deposition and investigate the interplay between the electrostatic and diffusion fields. We examine the effect of a local (nonuniform) flow field on deposition on a substrate.

PACS number(s): 68.70.+w, 82.20.Wt, 05.40.+j

Laplacian growth models such as diffusion-limited aggregation [1] (DLA) and its modifications give rise to a variety of morphologies which have been likened to patterns arising in several nonequilibrium growth processes [2]. Examples include dendritic solidification [3,4], directional solidification [5,6], electrodeposition [7–9], and Saffman-Taylor fingering [10,11]. Dendritic crystal growth processes are described by the diffusion equation which, in the quasistatic limit, reduces to the Laplace equation [4]. This approximation is singular in the sense that the significant coupled factors of a time and concentration dependence, and a finite-range diffusion field, vanish from the formulation. The description of an electrodeposition process by a Laplacian growth model [10] incorporates several simplifications including the assumption of local electroneutrality [12]. Recent experimental results [13] show that local departures from electroneutrality play a strong role in the growth of metal deposits. Clearly the use of models based on the Laplace equation to describe irreversible growth processes may yield a significant oversimplification. Another complication arising in growth processes occurs when the particles' trajectories are influenced by an imposed field. An example is deposition from a flowing fluid. Previous investigations [14–17] use biased random walker algorithms to study the effect of a uniform drift on deposition processes. These models are not readily shown to correspond to the continuum convection-diffusion equations.

In this article we develop a formal method for assigning rules to lattice-based walkers which are consistent with the general continuum equations describing a growth process. The rules governing the motion of walkers are derived from a finite difference scheme. This method allows the modeling of growth processes governed by partial differential equations (PDE's) more general than the Laplace equation. We first use the method to develop a lattice-based walker model to study diffusive growth in a finite concentration field. On introducing a parameter to reduce noise in the growth process, we show that the resultant patterns generated by the model are in agreement with analytical results. We then apply the method to the study of electrochemical deposi-

tion (ECD) and to deposition in a hydrodynamic flow.

The effect of a finite concentration field on aggregate growth was recently studied [18,19]. In contrast to Laplacian growth the patterns evolved with a constant velocity and became dense above a characteristic length scale related to the diffusion length  $l = 2D/v$ . The patterns exhibit a disordered structure due to the noise inherent in the growth algorithm. To model dendritic crystal growth one must systematically reduce this noise. We introduce noise reduction [3,11,20] into the finite concentration aggregation model and consider the relationship of the model to a finite difference scheme for the diffusion equation. This allows a quantitative comparison to be made with continuum based models of diffusive growth.

Although the lattice rules for the motion of a walker in aggregation models are generally introduced *a priori*, the rules here are *derived* from the finite difference equation to demonstrate the general method used in this paper. A finite difference scheme for solving the diffusion equation in two dimensions is

$$\frac{c_{i,j}^{t+\Delta t} - c_{i,j}^t}{\Delta t} = \frac{D(c_{i+1,j}^t + c_{i-1,j}^t + c_{i,j+1}^t + c_{i,j-1}^t - 4c_{i,j}^t)}{(\Delta x)^2}, \quad (1)$$

where  $c_{i,j}^t = c(x_i, y_j, t)$  is the number of particles per unit volume,  $D$  is the diffusion coefficient, and  $\Delta x = \Delta y$ . An analogous equation can be written for a Monte Carlo process. Defining  $p_{i,j}^t = (\Delta x)^3 c_{i,j}^t$  to represent the number of particles at each lattice site, taking one time step as equal to  $\Delta t$  and defining  $\bar{D} = D \Delta t / (\Delta x)^2$ , (1) can be rewritten as

$$p_{i,j}^{t+1} = (1 - 4\bar{D})p_{i,j}^t + \bar{D}(p_{i+1,j}^t + p_{i-1,j}^t + p_{i,j+1}^t + p_{i,j-1}^t). \quad (2)$$

The clear physical interpretation of this equation is that the contribution to the particles at site  $i, j$  at time  $t + 1$  is from particles at the site itself and its surrounding neighbors at time  $t$ . This relationship defines the rules governing the motion of walkers at each site:  $(1 - 4\bar{D})p_{i,j}^t$  remain at the site, while  $\bar{D}p_{i,j}^t$  step to each of the neighbors. The prefactors in these expressions can be interpreted as probabilities governing the motion of individual

particles.

It should be noted that the discretization [Eq. (1)] of the diffusion equation is not unique. The only constraint on the choice is that the probabilities associated with each of the actions of walkers be greater than zero. Equation (1), and subsequent discretizations, are therefore chosen for simplicity. We do not expect the choice of discretization to affect the overall properties of the model.

Using the rules defined by (2) for the motion of walkers, simulations are performed in a rectangular cell of width  $L$  with periodic boundary conditions imposed laterally. A finite concentration field is simulated at height  $H$  by maintaining the average occupancy of these sites at  $p$  walkers per lattice site. When a particle strikes a surface site (a site adjacent to the cluster) it is absorbed by the cluster. Noise reduction at the growing interface is implemented by accumulating particles at surface sites, until the total reaches  $m$ , whereupon the site is filled. Although the parameter was originally introduced to reduce noise [3,11,20] in the DLA model, it has a clear interpretation as the inverse of the volume of the diffusing particles. In fact, the parameters  $p$ ,  $m$ , and  $\bar{D}$  of the model can be related to physical parameters by the relationship of the model to the finite difference scheme.

In the limit of this model as  $p, m \rightarrow \infty$  such that  $\Delta = p/m$  remains finite, the distribution of walkers from one time step to the next is given exactly by the finite difference equation (1). The proportion of a surface site filled per time step (the interfacial velocity) is given by  $\bar{v} = \bar{D} \sum_{NN} \nabla p_{i,j}^t / m$  where the summation is over the nearest neighbors to the surface site. In this limit the model is similar to the algorithm of late stage crystal growth based on a cell dynamical scheme [21]. As  $\Delta \rightarrow 0$  the algorithm for deterministic Laplacian growth [22,23] is recovered.

We compare morphologies generated by our model in the deterministic limit (the field scaled by a factor  $m$ ) with three analytic results. The relevant boundary conditions are  $p = 0$  and  $\mathbf{v} \cdot \mathbf{n} = \bar{D} \nabla p \cdot \mathbf{n}$  at the interface, where  $\mathbf{v}$  is the velocity and  $\mathbf{n}$  is the unit normal directed outward from the cluster. Far from the interface  $p = \Delta$ . In one dimension a similarity solution exists which satisfies the initial condition  $p(x, 0) = \Delta$  for  $x > 0$ . The position of the growing interface is given by  $X(t) = \beta \sqrt{t}$  [24] where  $\beta$  satisfies

$$\Delta = \sqrt{\pi} \beta \exp(\beta^2) \operatorname{erfc} \beta. \quad (3)$$

The values of  $\beta$  determined from the lattice-walker model are shown along with the theoretical result in Fig. 1. The agreement is excellent. In two dimensions the Ivantsov parabola [25] provides a method of comparison. The parabola advances with constant velocity  $v$  and tip radius  $\rho$ . The relationship between the dimensionless Peclet number  $Pe = v\rho/2D$  and the bath concentration is given by an equation analogous to (3),

$$\Delta = \sqrt{\pi} \sqrt{Pe} \exp(Pe) \operatorname{erfc} \sqrt{Pe}. \quad (4)$$

The tip radius and velocity are estimated by a least-squares fit to the advancing interface. The Peclet number

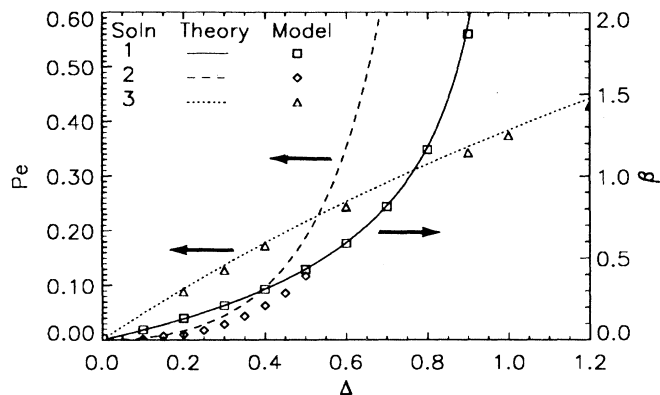


FIG. 1. Comparisons of morphologies generated by the deterministic lattice-walker model with analytical predictions. (1) One-dimensional interface; (2) Ivantsov parabola; (3) modified model.

is plotted against its theoretical value in Fig. 1. An example of the least-squares fit for  $\rho$  is shown in Fig. 2(a). The behavior is qualitatively correct and the results of the model are of the right order. The breakdown of the solution appears to be due to the dominance of lattice effects, which strongly bias tip sites. Note that (4) does not uniquely determine  $\rho$  or  $v$ , but only their product [26]. In the conventional analysis, anisotropic surface tension is needed to select a unique tip radius [25,27]. Interfaces in diffusion-controlled growth are unstable on all length scales if there is no surface tension, therefore the scale of the growth for a given discretization is largely determined by the lattice spacing.

These lattice effects can be avoided by modeling a solution which has a characteristic length scale greater than that of the underlying lattice. Such a solution is obtained by reversing the sign of the moving boundary condition and defining  $p = \Delta$  for  $x = 0$  and  $z \in (-\infty, vt]$ , and  $p = 0$  for  $z > z_i$  where  $z_i = \rho/2 - x^2/2\rho + vt$  is the position of the interface. In this case  $v$  is a parameter, and  $\rho$  is determined by a relation for  $Pe$ :

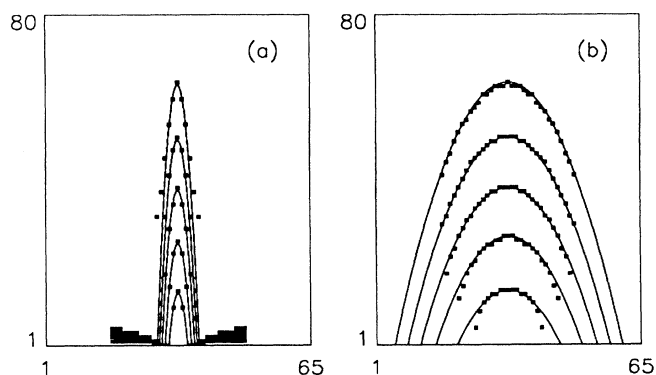


FIG. 2. Example of a least-squares fit for the average interface profile at uniform time intervals. (a) needle crystal; (b) the modified model.

$$\Delta = \sqrt{\pi} \sqrt{\text{Pe}} \exp(\text{Pe}) \text{erf} \sqrt{\text{Pe}}. \quad (5)$$

By reducing  $v$ , the characteristic length scale  $\rho$  is increased. This solution can be readily simulated by (i) changing the boundary conditions of the model so that sites on the  $x$  axis with  $z < vt$  are held at concentration  $\Delta$  and (ii) modifying the growth rule of the algorithm so that a cluster site becomes a field site after it has accumulated  $m$  walkers. An example of a fully developed parabola is given in Fig. 2(b) and the results of the model are compared with the theoretical values in Fig. 1. The consistent agreement with analytic results gives us confidence that the method for assigning rules to lattice-based walkers is well founded and able to reproduce morphologies realized in other physical systems.

Experimental studies of electrochemical deposition have led to the identification of several morphologies (DLA-like, dense branching morphology, and dendritic) [9] dependent on the experimental conditions. Several mechanisms have been proposed to explain the large range of morphologies. A hypothesis for the respective roles of the Laplacian and the diffusion fields has been given [28,29] and electrochemical aspects of the problem

such as departures from electroneutrality have been studied experimentally [12]. We numerically model ECD and study the interplay between the electrostatic field and the diffusion field, and consider the effects of screening on the growth morphology.

Neglecting convection of the electrolyte the equations governing the concentration fields of ions ( $c_{\pm}$ ) in ECD are

$$\frac{\partial c_{\pm}}{\partial t} = -\nabla \cdot \mathbf{j}_{\pm}, \quad (6)$$

$$\mathbf{j}_{\pm} = -D \nabla c_{\pm} \mp \mu c_{\pm} \nabla \phi, \quad (7)$$

where  $\mathbf{j}_{\pm}$  denotes the ion flux,  $\phi$  the electrostatic potential,  $D$  the diffusion coefficient, and  $\mu$  the ionic mobility. The electrostatic potential is determined by the solution to the Poisson equation:

$$\nabla^2 \phi = -\frac{e}{\epsilon} (z_+ c_+ - z_- c_-). \quad (8)$$

The rules governing the motion of the walkers which are consistent with (6) and (7) are determined from

$$\begin{aligned} p_{i,j}^{t+1} = & p_{i,j}^t \left[ 1 - 4\bar{D} + \frac{\bar{k}}{2} \nabla_d^2 \phi \right] + p_{i+1,j}^t \left[ \bar{D} + \frac{\bar{k}}{2} (\phi_{i+1,j} - \phi_{i,j}) \right] p_{i-1,j}^t \left[ \bar{D} - \frac{\bar{k}}{2} (\phi_{i,j} - \phi_{i-1,j}) \right] \\ & + p_{i,j+1}^t \left[ \bar{D} + \frac{\bar{k}}{2} (\phi_{i,j+1} - \phi_{i,j}) \right] + p_{i,j-1}^t \left[ \bar{D} - \frac{\bar{k}}{2} (\phi_{i,j} - \phi_{i,j-1}) \right], \end{aligned} \quad (9)$$

where  $\bar{k} = \mu \Delta t / (\Delta x)^2$ . There is experimental [12,13] and theoretical evidence [30] of the existence of a charged region with an associated potential drop near the tips of the growing deposit. The screening at the tips can be simply incorporated into the ECD model by replacing (8) with

$$\nabla^2 \phi = \lambda^2 \phi, \quad (10)$$

where  $\lambda^{-1}$  is a length scale describing the extent of the charged region.

Numerical simulations are performed in rectangular cells of width  $L = 256$ , the clusters grown to a height of 350. A constant potential drop is imposed across the cell, the potential at the upper boundary ( $H = 1000$ ) of the cell being fixed at zero. Varying  $p$  and  $\lambda^{-1}$  allows one to study the interplay of the length scales associated with the diffusion and electric fields. The emergent length scales of the growth morphologies are simplest to discern for a high noise reduction parameter. We show in Fig. 3 numerical results for various  $p$  and  $\lambda^{-1}$  where  $m = 8$ . At

large concentration (small diffusion length  $l$ )  $\lambda^{-1}$  determines the spacing between parallel needles. Figures 3(a)–3(c) show that the spacing increases with  $\lambda^{-1}$ . At lower concentrations (large  $l$ ) the diffusion field determines the spacing between the needles [see Fig. 3(d)]. The selection of the characteristic distance between needles is clearly determined by the largest screening length.

There have been several recent studies examining the influence of fluid flow on growth morphology [12,14–16,31,32]. In most previous studies the complex fluid motion was replaced by a uniform flow. We examine the effect of a local flow configuration on the morphology. The equation governing the concentration field is again (6), with the flux term now given by

$$\mathbf{j} = -D \nabla c + c \mathbf{u}, \quad (11)$$

where  $\mathbf{u}$  is the local velocity field. The equation describing the evolution of the probability field of walkers defined by (6) and (11) is

$$\begin{aligned} p_{i,j}^{t+1} = & p_{i,j}^t \left[ 1 - 4\bar{D} - \frac{1}{2} \bar{u}_{i+1/2,j}^t + \frac{1}{2} \bar{u}_{i-1/2,j}^t - \frac{1}{2} \bar{u}_{i,j+1/2}^t + \frac{1}{2} \bar{u}_{i,j-1/2}^t \right] + p_{i+1,j}^t \left[ \bar{D} - \frac{1}{2} \bar{u}_{i+1/2,j}^t \right] \\ & + p_{i-1,j}^t \left[ \bar{D} + \frac{1}{2} \bar{u}_{i-1/2,j}^t \right] + p_{i,j+1}^t \left[ \bar{D} - \frac{1}{2} \bar{u}_{i,j+1/2}^t \right] + p_{i,j-1}^t \left[ \bar{D} + \frac{1}{2} \bar{u}_{i,j-1/2}^t \right]. \end{aligned} \quad (12)$$

The local flow field is then given by the solution to the Navier-Stokes equations. A good approximation to the flow field can be obtained by solving the equations for potential flow [33]. We introduce the velocity potential,  $\phi(x,y)$  defined by  $u_x = -\partial \phi / \partial x$ ,  $u_y = -\partial \phi / \partial y$ ; for two-dimensional irrotational flow  $\phi$  satisfies the Laplace equation. The velocity terms defined in (12) are given by the gradient of the potential [e.g.,  $\bar{u}_{i+1/2,j} = -(\phi_{i+1,j} - \phi_{i,j})$ ].

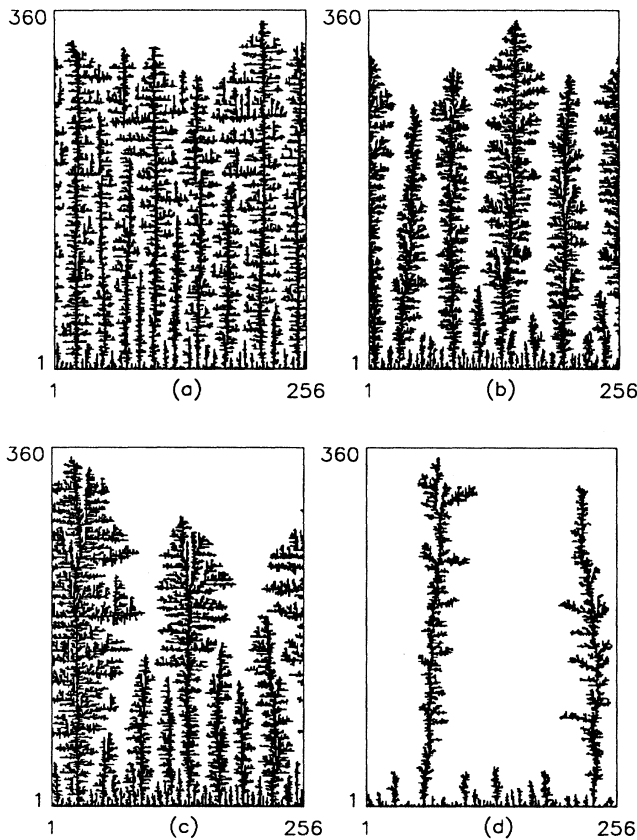


FIG. 3. The effect of varying the screening lengths of the diffusion and electrostatic fields. (a)  $p/m = 0.4$ ,  $\lambda^{-1} = 0$ ; (b)  $p/m = 0.4$ ,  $\lambda^{-1} = 10$ ; (c)  $p/m = 0.4$ ,  $\lambda^{-1} = 25$ ; (d)  $p/m = 0.1$ ,  $\lambda^{-1} = 10$ .

Previous studies of deposition on a surface in the presence of a uniform drift yield clusters that are strongly inclined toward the incoming flow field [16] [see Fig. 4(a)]. We simulate this deposition process on a plate at the base of a square lattice with side length 200. A constant velocity (parallel to the plate) and concentration were maintained along the perimeter of the cell, and zero normal velocity was imposed at the cluster surface. The walkers stick irreversibly to the cluster, their motion in the field

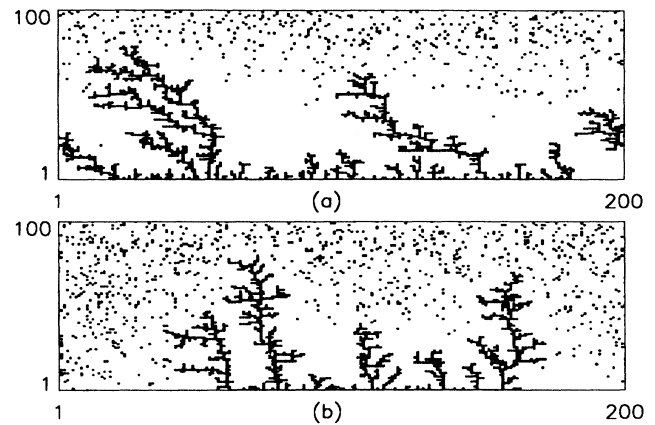


FIG. 4. Effect of a local flow field on deposition in a hydrodynamic flow. Clusters grown from a substrate in (a) uniform flow field; (b) a local flow field.

governed by (12). The effect of the local flow field on the cluster morphology is dramatic. The clusters grow vertically from the plate with little tendency to grow upstream [see Fig. 4(b)]. In the radial geometry [14] clusters grown from a seed in a uniform flow field had a strong tendency to grow in the quadrant directed upstream. This effect was not seen when a local field was incorporated.

Extensions of our method include the incorporation of surface tension into the deterministic model. This will reduce lattice effects, and may provide an alternative to the current schemes implemented in the numerical study of dendritic crystal growth [21,34]. A comprehensive study of ECD and using more realistic interfacial boundary conditions is underway. Recent experimental results show that charge at the tips of the aggregate can lead to convective motion of the fluid [13]—we shall utilize the method described above to study the effect of convection on ECD. The model of convection diffusion deposition can be generalized to include viscous flow and may be appropriate for studying certain biological processes and engineering problems.

The authors wish to acknowledge valuable discussions with M. N. Barber.

- 
- [1] T. A. Witten and L. M. Sander, *Phys. Rev. B* **27**, 5686 (1983).
  - [2] H. E. Stanley *et al.*, *Physica A* **168**, 23 (1990).
  - [3] J. Nittman and H. E. Stanley, *Nature (London)* **321**, 663 (1986).
  - [4] J. Szép, J. Cserti, and J. Kertész, *J. Phys. A* **18**, L413 (1985).
  - [5] A. Karma, *Phys. Rev. Lett.* **59**, 71 (1987).
  - [6] S. K. Sarkar and M. H. Jensen, *Phys. Rev. A* **35**, 1877 (1987).
  - [7] M. Matsushita, M. Sano, Y. Hayakawa, and H. Honjo, *Phys. Rev. Lett.* **53**, 286 (1984).
  - [8] F. Argoul, A. Arneodo, and G. Grasseau, *Phys. Rev. Lett.* **61**, 2558 (1988).
  - [9] D. Grier, E. Ben-Jacob, R. Clarke, and L. M. Sander, *Phys. Rev. Lett.* **56**, 1264 (1986).
  - [10] A. Arneodo, Y. Couder, G. Grasseau, V. Hakim, and M. Rabaud, *Phys. Rev. Lett.* **63**, 984 (1989).
  - [11] C. Tang, *Phys. Rev. A* **31**, 1977 (1985).
  - [12] V. Fleury, M. Rosso, J.-N. Chazalviel, and B. Sapoval, *Phys. Rev. A* **44**, 6693 (1991).
  - [13] V. Fleury, J.-N. Chazalviel, and M. Rosso, *Phys. Rev. Lett.* **68**, 2492 (1992).
  - [14] P. Meakin, *Phys. Rev. A* **28**, 5221 (1983).
  - [15] R.-F. Xiao, J. W. D. Alexander, and F. Rosenberger, *Phys. Rev. A* **38**, 2447 (1988).

- [16] T. Nagatani and F. Sagues, *Phys. Rev. A* **43**, 2970 (1991).
- [17] S. Seki, M. Uwaha, and Y. Saito, *Europhys. Lett.* **14**, 397 (1991).
- [18] R. F. Voss, *Phys. Rev. B* **30**, 334 (1984).
- [19] M. Uwaha and Y. Saito, *Phys. Rev. A* **40**, 4716 (1989).
- [20] J. Kertész and T. Vicsek, *J. Phys. A* **19**, L257 (1986).
- [21] F. Liu and N. Goldenfeld, *Phys. Rev. A* **42**, 895 (1990).
- [22] P. Garik, R. Richter, J. Hautman, and P. Ramanial, *Phys. Rev. A* **32**, 3156 (1985).
- [23] M. T. Batchelor and B. I. Henry, *Phys. Rev. A* **45**, 4180 (1992).
- [24] J. Crank, *Free and Moving Boundary Problems* (Clarendon, Oxford, 1984).
- [25] A. Barbieri, D. C. Hong, and J. S. Langer, *Phys. Rev. A* **35**, 1802 (1987).
- [26] This is consistent with the model as the following argument shows. Denoting unscaled quantities with subscript  $u$  the pattern for a given discretization is characterized by  $\rho_u = \rho \Delta x$  and  $v_u = v \Delta x / \Delta t$ . Choosing the discretization  $\Delta x' = a \Delta x$  and  $\Delta t' = a^2 \Delta t$  does not change  $\rho$  or  $v$ , since  $\Delta' = \Delta$  and  $D' = D$ . Therefore  $\rho'_u = a \rho_u$  and  $v'_u = v_u / a$ , which demonstrates the degeneracy of the model.
- [27] D. A. Kessler, J. Koplik, and H. Levine, *Phys. Rev. A* **33**, 3352 (1986).
- [28] P. Garik *et al.*, *Phys. Rev. Lett.* **62**, 2703 (1989).
- [29] E. Louis, F. Guinea, O. Pla, and L. M. Sander, *Phys. Rev. Lett.* **68**, 209 (1992).
- [30] J.-N. Chazalviel, *Phys. Rev. Lett.* **42**, 7355 (1990).
- [31] Y. Hayakawa, S. Sato, and M. Matsushita, *Phys. Rev. A* **36**, 1963 (1987).
- [32] J.-C. Toussaint, J.-M. Debierre, and L. Turban, *Phys. Rev. Lett.* **68**, 2027 (1992).
- [33] R. B. Bird, W. E. Stewart, and E. N. Lightfoot, *Transport Phenomena* (Wiley, New York, 1960).
- [34] J. A. Sethian and J. Strain, in *On the Evolution of Phase Boundaries*, edited by M. E. Gurtin and G. B. McFadden (Springer-Verlag, Berlin, 1992).